

A NEW TYPE OF RF ELECTRON ACCELERATOR: THE RHODOTRON

Jacques POTTIER

CEA/IRDI/D. LETI/DEIN, 91191 Gif-sur-Yvette Cedex, France

In the median plane of a cavity resonator derived from a $\lambda/2$ coaxial line short-circuited at both ends the magnetic field is zero and the electric field is radial. Therefore it is possible to accelerate charged particle beams crossing diametrically the cavity within this plane without parasitic deflections. By appropriate bending of the beam outside of the cavity by magnets, n successive accelerations are performed, so that the shunt-impedance is increased by a factor of n^2 . Optimization of the shunt-impedance achieved by taking into account the phase stability conditions determines the dimensions of the device for a given n . Proper shaping of the magnet edges produces a suitable focussing. Such a machine, a prototype of which is under completion, turns out to be very convenient for accelerating 20–500 kW electron beams to energies in the 1–20 MeV range.

1. Introduction

Bending a charged particle beam so that it may be accelerated several times by the same field is not a new idea. It accounts for the design of cyclic machines (such as the cyclotron, the synchrotron, and the microtron) in which the successive trajectories are not kept apart, which leads to some difficulties (for instance, drastic limitation of the current due to strong space-charge effects).

Actually, it has been proposed to perform n distinct passes in the same accelerating cavity in order to increase the energy n times [1].

However, with cylindrical cavities in common use, there is no magnetic component of the field along the axis, but everywhere else there is a magnetic component (fig. 1). For trajectories outside the axis, electrons are deviated by the field according to its phase, which prevents correct operation. So other types of cavities are required. In a coaxial $\lambda/2$ line, short-circuited at both ends (fig. 2), the radial E field is maximum in the

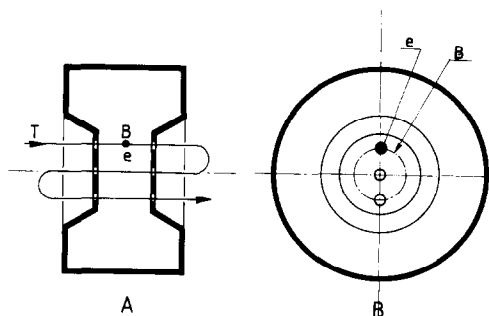


Fig. 1. (a) Axial section, (b) median section. In cavities commonly used, an electron trajectory T outside the axis encounters a transverse magnetic field B .

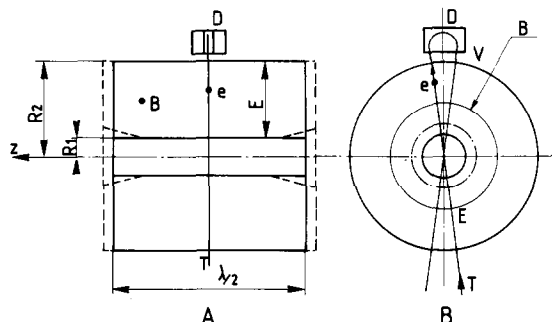


Fig. 2. (a) Axial section, (b) median section. Coaxial cavity. Dotted lines: Improved shunt-impedance cavity. Magnetic field B is zero in the median plane. Electron trajectory T is not perturbed. D: open V faced deflecting magnet. E: electric field.

median plane, whereas the azimuthal B field is zero. By properly bending the beam outside the cavity by deflectors D , n successive accelerations along diametrical trajectories may be carried out. This structure affords a very promising solution to the problem because of its high shunt-impedance and its mechanical properties. It is easy to build, its outer cylinder is well suited for sustaining the atmospheric pressure, and its inner cylinder helps the terminal flanges from bending.

2. Basic theory

2.1. Shunt-impedance

The shunt-impedance is $Z_s = V^2/P$, where

$$V = 2 \int_{R_1}^{R_2} |E| dr$$

and P is the dissipated power.

The field distributions may be written in the form

$$E = \frac{E_0}{r} \cos \frac{2\pi z}{\lambda} \sin(\omega t + \phi),$$

$$B = \frac{B_0}{r} \sin \frac{2\pi z}{\lambda} \cos(\omega t + \phi),$$

and through the induction law $V = \omega \iint B \, ds$, the current distribution may be easily derived and hence P and the shunt-impedance:

$$Z_s = \frac{8\pi}{\rho_s} 60^2 \ln^2 \frac{R_2}{R_1} \left(\frac{\lambda}{8} \left(\frac{1}{R_1} + \frac{1}{R_2} \right) + \ln \frac{R_2}{R_1} \right)^{-1}, \quad (1)$$

where ρ_s is the areal skin effect resistivity. For copper, $\rho_s = 2.51 \times 10^{-7} \, \Omega^{1/2}$.

In fact, E does not remain equal to $|E|$ during a pass: the useful parameter is the effective shunt-impedance $Z_{se} = Z_s T^2$ where T is the transit time factor.

2.2. Transit time factor

A supposed relativistic electron crossing the axis at time 0 (fig. 3) is the most accelerated. The E field may be written as

$$E = \frac{E_0}{r} \sin \theta,$$

with $\theta = \omega t$ and

$$T = \int_{R_1}^{R_2} \frac{\sin \theta}{r} dr / \int_{R_1}^{R_2} \frac{1}{r} dr.$$

As $\theta = 2\pi r/\lambda$, $r = (\lambda/2\pi)\theta$, one obtains

$$T = \frac{S_i \theta_2 - S_i \theta_1}{\ln \theta_2 / \theta_1}, \quad (2)$$

with

$$S_i(\theta) = \int_0^\theta \frac{\sin \theta}{\theta} d\theta.$$

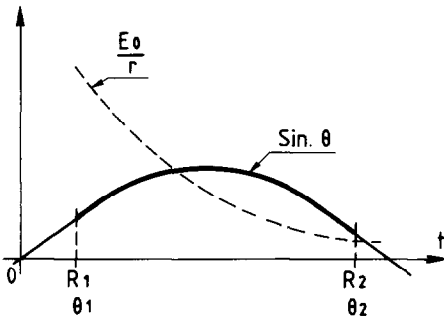


Fig. 3. Transit time factor. For a relativistic electron crossing the axis at time 0, the electric field is $E_0/r \sin \theta$ with $\theta = \omega t = 2\pi r/\lambda$.

For electrons crossing the axis at $t_0 \neq 0$, $\omega t_0 = \phi$ and T has to be multiplied by $\cos \phi$.

2.3. Synchronism conditions – phase stability

The trajectory length between two successive passes through the axis must be an integer number p of λ . It includes the bending path outside the cavity, somewhat greater than πR_c , R_c being the curvature radius.

R_c cannot be made too small: this would imply a gap thinner than the beam, and in some cases a too strong induction in the magnets. R_c decreases as n increases: there is an upper limit to n . $n = 6$ appears as a very conservative value in a number of cases, and $n = 12$ and beyond seems feasible.

R_c defines R_2 : Taking into account the distance of the magnets from the cavity required for fringing fields and the thickness of the outer cylinder, for $n = 6$ for instance, leads to $R_2 \approx 0.27\lambda$.

Phase stability is of the relativistic synchrotron type instead of the linac one: as R_c increases with the energy, the greater the energy, the longer the trajectory. Therefore, the energy gain must be less for later electrons: the stability domain corresponds to $\phi > 0$. The synchronous electron must present a phase lag ϕ_s , about 15° , entailing an energy dispersion much smaller than the one obtained with a linac.

2.4. Effective shunt-impedance Z_{se} optimization

Two cases are of interest: $p = 2$, for which an absolute maximum of Z_{se} is obtained for $R_2 \approx 0.5\lambda$; and $p = 1$, for which the dimensions are minimized, the relative maximum of Z_{se} being obtained for the largest convenient R_2 value, for instance $R_2 \approx 0.27\lambda$ for $n = 6$.

Optimization results are summarized in table 1.

The theoretical value of Z_{se} may be improved by about 10%, as shown by SUPERFISH simulations, by using appropriate truncated cone terminations of the inner cylinder (fig. 2), the cavity being then somewhat longer than $\lambda/2$. Besides, measured shunt-impedances are as a rule 25% lower than the computed values, so that $Z_{sp} = 0.85Z_{se}$ is taken in table 1 as the practical value of the effective shunt-impedance of an improved cavity.

Table 1
Optimized characteristics

P	R_2 (m)	R_1/R_2	Z_{se} (M Ω)	Z_{sp} (M Ω)
1	0.27λ	$1/4$	$5.77\lambda^{1/2}$	$4.9\lambda^{1/2}$
2	0.5λ	$1/7$	$10.4\lambda^{1/2}$	$8.83\lambda^{1/2}$

Table 2
Energy W (MeV) for $P=100$ kW and $f=130$ MHz

R_2 (m)	2	3	4	5	6	7	8	9	10	11	12
0.62	1.8	2.7	3.6	4.5	5.4	6.3	7.2	8.1	9	9.9	10.8
1.15	2.4	3.6	4.8	6	7.2	8.4	9.6	10.8	12	13.2	14.4

3. Energy range – beam power

The energy gain per pass is:

$$W_1 = Z_{sp}^{1/2} P^{1/2} \cos \phi.$$

Taking $\phi = 15^\circ$ and Z_{sp} given by table 1, leads to a total energy for n passes:

$$\begin{aligned} W &\approx 2.3\lambda^{1/4} P^{1/2} n & \text{for } R_2 = 0.27\lambda, \\ W &\approx 3.1\lambda^{1/4} P^{1/2} n & \text{for } R_2 = 0.5\lambda, \end{aligned} \quad (3)$$

W being expressed in MeV, P in MW. W is not very sensitive to λ . The volume being proportional to λ^3 , short wavelengths are beneficial.

Practically, frequencies in the 100–200 MHz range for which powerful tubes are available are to be chosen.

As an example, table 2 shows energies obtained for $P = 100$ kW, $f = 130$ MHz ($\lambda = 2.3$ m) according to the number n of passes, supposing $R_2 \approx 0.27\lambda$ whatever n may be.

The cavity being about 1.2 m long in both cases, is not much more cumbersome for $R_2 = 1.15$ m ($p = 2$) than for $R_2 = 0.62$ m ($p = 1$), but the outside diameter of the accelerator, including the magnets, would be about 5 m for $p = 2$ instead of 2.5 m for $p = 1$. The same energy is obtained for $[n(p = 1)]/[n(p = 2)] = 4/3$: the choice $p = 2$ is valuable only if high energies are needed.

The moderate power needed allows a c.w. operation without any pulse generator.

4. Focussing

An analysis of focussing problems involving space-charge effects is out of the scope of this short paper.

Numerical simulations have shown that, at least for practical cases studied, a good focussing is provided by a proper open V facing of the deflecting magnets without any auxiliary device.

5. Additional features

A single cavity is used, so that tuning may be performed by controlling the frequency through electronic means, and no mechanical device such as a stud in the cavity is required. The E_0/r law of the electric field makes the cavity probably relatively insensitive to the multipactor effect and lowers the E field at the input aperture, providing an easier injection.

The only requirement specific to this type of machine is to control within about 1% the rf level and the magnetic field of the deflectors.

6. Conclusion

With the proposed technique, compact, relatively inexpensive powerful electron machines suited for accelerating 20–500 kW beams to energies in the 1–20 MeV range, can be built.

A feasibility prototype with a vertical axis cavity is being completed. Its main characteristics are: $f = 180$ MHz, $P_{rf} = 70$ kW, $n = 6$, $R_1 = 0.1125$ m, $R_2 = 0.45$ m, cavity length = 0.916 m, outside diameter = 1.8 m, outside height = 2.1 m, beam energy = 3.3 MeV, beam power ≈ 20 kW.

I wish to thank Annick Nguyen, Jean-Pierre Gueguen and Krzysztof Umiastowski for their valuable help in this work.

Reference

- [1] Bernard Epsztein and Jacques Pinel, Accélérateur d'électrons de 10 MeV en régime permanent, C.S.F. patent n° 129 070, (23 Dec. 1968).